NUCL SCI TECH (2017) 28:2
DOI 10.1007/s41365-016-0155-x

In-situ high-energy-resolution X-ray absorption spectroscopy for UO_2 oxidation at SSRF

Pei-Quan Duan[1] · Hong-Liang Bao[1] · Jiong Li[1] · Han-Jie Cao[1] · Yu-Ying Huang[1]

Received: 8 March 2016 / Revised: 26 April 2016 / Accepted: 12 May 2016 / Published online: 30 November 2016

Abstract Based on the high-energy-resolution fluorescence spectrometer on the BL14W1 beamline at Shanghai Synchrotron Radiation Facility, an in-situ high-energy-resolution X-ray absorption spectroscopy technique, with an in-situ heating cell, was developed. The high-energy-resolution fluorescence detection for X-ray absorption near-edge spectroscopy (HERFD-XANES) was tested in a UO_2 oxidation experiment to measure the U L_3-edge, with higher signal-to-noise ratio and higher-energy-resolution than conventional XANES. The technique has potential application for in-situ study of uranium-based materials.

Keywords X-ray absorption spectroscopy (XAS) · In-situ cell · UO_2 oxidation

1 Introduction

As a general nuclear fuel, uranium dioxide has been studied for 50 years, being concentrated on oxidation under different temperatures, oxygen pressure and so on [1]. Temperature is the main condition of oxidation process. Properties of the oxidation products change distinctively with temperature, such as the chemical valence, electronic structure and crystal structure. As temperature increases, UO_2 with a fluorite crystal type forms a series of mixed-valence oxidation products: $U_3O_7/U_4O_9,U_3O_8$ [2]. This process occurs in the nuclear fuel cycle, transport and waste disposal, with a risk of the volume increase. For example, the final oxidation product U_3O_8 has a 36% net volume increase over UO_2 due to remarkable difference in crystalline structure and the decreased U/O ratio. To avoid this risk, the uranium dioxidation processes under different temperatures should be studied in advance. X-ray absorption near-edge spectroscopy (XANES) in fluorescence mode is an advanced technique for acquiring information about the chemical valence state and electronic structure of actinide elements. XANES requires not much on the probed samples, and its high penetrating power allows bulk detection and in-situ measurement [3]. For detecting valence state of L-edge of actinide elements, however, conventional XANES is limited by the excessively broad spectra width originating from the short 2p core-hole lifetime.

By collecting the Lα emission line, high-energy-resolution fluorescence detection for X-ray near-edge absorption spectroscopy (HERFD-XAS) performs much better in energy resolution than conventional XAS. HERFD-XAS stations have been established worldwide in increasing numbers [4] during the past two decades, and in the recent years, several groups began their efforts of using this method to study chemical states and electronic structure of actinide elements [5, 6]. The broad width of L_3-edge HERFD-XAS at Lα line originating from the core-hole lifetime of 3d is longer than 2p, so some details of the spectra could be extracted [7]. The white line of XAS could provide the information of unoccupied 6d states. The shift of white line is limited to the spectrum width, and narrow white line of HERFD-XAS could obtain more precise

---

This work was supported by the National Nature Science Foundation of China (Nos. 11175244 and U1532259).

✉ Yu-Ying Huang
huangyuying@sinap.ac.cn

[1] Shanghai Synchrotron Radiation Facility, Shanghai Institute of Applied Physics, Chinese Academy of Sciences, Shanghai 201204, China

structure or the small variation of 6d states [8, 9]. Furthermore, most of the chemical properties of actinide are related to the 5f states [10]. The pre-edge peaks of actinide elements HERFD-XAS originating from transition from 2p to 5f could provide the information of valence state of 5f [11]. Vitova et al. [12] studied different valences of uranium oxides. The HERFD-XAS of three standard samples illustrated the difference between U^{4+}, U^{5+} and U^{6+}. The energy resolution at U L_3 of conventional XAS is about 14 eV, while it was 9 eV for HERFD-XAS. This improved energy resolution provided precise analysis about valence changes.

The energy resolution power of U L_3 HERFD-XAS is limited by energy resolution of the incident beam, the spectrometer and the nature broadening related to the lifetime of 3d core hole. The nature broadening of uranium $M_{4,5}$-edge is about 3 eV, so the energy resolution of U L_3 HERFD-XAS must be better than 3 eV. Under these conditions, the chemical shift (<3 eV) cannot be detected by L_3-edge HERFD-XAS. Therefore, the HERFD-XAS of U M_4-edge with high energy resolution [13] was developed. The X-ray of U M_4-edge is too soft to penetrate the gas atmosphere in in-situ study [14], so the hard X-ray of U L_3-edge, of good penetrability, is suitable for the HERFD-XAS technique in in-situ environment. A high-resolution X-ray fluorescence spectrometer based on Rowland circle geometry on BL14W1 at SSRF has been established [15] for X-ray emission spectroscopy and HERFD-XANES.

In this paper, HERFD-XANES data of U L_3-edge with high signal-to-noise for UO_2 oxidation are obtained, by using the in-situ high-energy-resolution X-ray absorption spectroscopy with an in-situ heating cell.

2 Experiments

The crystal structures of the UO_2 sample before and after in-situ oxidation were characterized with powder X-ray diffraction (XRD) on a Bruker D8 Advance X-ray diffractometer using the Ni-filtered Cu Kα radiation source at 40 kV and 40 mA, performed on the BL14W1 beamline at SSRF [16]. The incident beams were from a pair of Si(311) reflection crystal monochromator. Little mismatch of the monochromator was performed for the rejection of higher harmonics. The flux at the sample position could reach to 3×10^{12} photos/s. The energy calibration was achieved at Zr-L3 absorption edge (17998 eV). As shown in Fig. 1a, the sample was placed in the in-situ heating cell, and the centers of the cell, crystal and detector were on the Rowlan circle. The X-ray beams were from a bending crystal Ge(777) (1 m in curvature radius), and the energy resolution could be down to 2.4 eV with the convolution of incident energy. The XANES spectra were scanned from 17,155 to 17,250 eV in 0.3 eV steps around white line. The emission spectrometer was performed for HERFD-XAS and resonant X-ray emission spectrum. The conventional XAS (total fluorescence yield XAS TFY-XAS) was acquired by a gas chamber at transition mode. The UO_2 powder, fabricated by China North Nuclear Fuel Company Limited, was annealed for 6 h under 5% H_2 and Ar atmosphere at 1273 K, to ensure that the composition of UO_2 powder was stoichiometric. The UO_2 powder was oxidized to U_3O_8 in air. Two standard samples (UO_2 and U_3O_8) were used as the reference. The sample UO_2 was powdered in order to accelerate the oxidation process. Two asbestine cylinders were used to clamp the powder sample and reduce absorption of the incident X-ray. The in-situ cell then was placed at the intersection of X-ray line and Rowland circle. The heating apparatus contains two probes inside the cell and a temperature controller that alters and maintains the temperature at the sample position. The cell has two more probes to provide 100% O_2 gas and pure He gas as protective gas. The entire cell was water cooled (Fig. 1b). The sample UO_2 was heated to 300, 470, 520, 620, 770 and 970 K at O_2 atmosphere and kept at each temperature for 1 h. Then, the HERFD-XAS was acquired at pure He atmosphere to ensure the oxide reaction no longer proceeded.

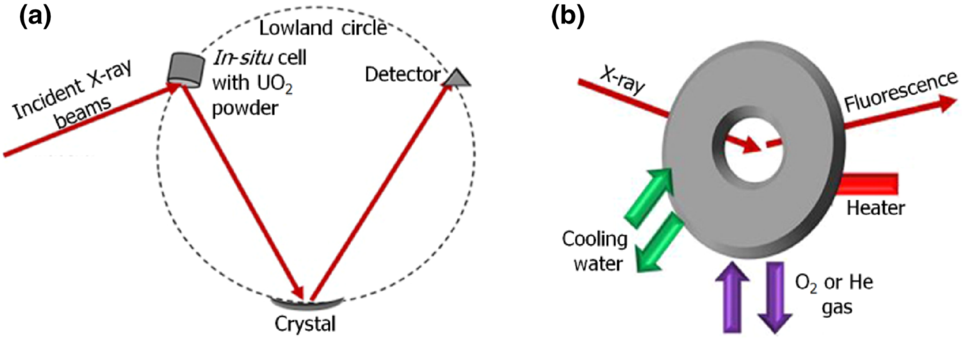

Fig. 1 Priciple of the HERFD-XAS spectrometer (**a**) and the in-situ cell (**b**)

3 Results and discussion

The spectra of HERFD-XAS and conventional XAS (TFY) of UO_2 at room temperature are shown in Fig. 2a. The full width at half maximum (FWHM) of peaks A and B for TFY-XAS is 14 and 7 eV, respectively, while it is 9 and 6 eV, respectively, for HERFD-XAS. Peak A is the white line. It is sensitive to the variation of valence state, and its shift provides information about valence state of oxidation products. Peak B originates from multiple scatting, and the distance between A and B is inversely proportional to lattice spacing. So, the more narrow peaks, the more precise lattice spacing will be obtained [17]. U_3O_8 forms via mixed-valence oxidation, and peaks A and B of U_3O_8 are wider than those of UO_2. The HERFD-XAS of UO_2 and U_3O_8, as standard samples, is shown in Fig. 2b. The peak intensities decreased gradually and the width increased. The intensity decrease in the main peaks could be due to the damaged symmetry of crystalline structure by the added O atoms [18, 19]. And the broadened main peaks could be originated from the combination of two valences of U_3O_8 [20]. The spectrum of U_3O_8 has a distinct shoulder peak at the higher energy side, due to multiple scattering.

Figure 3 shows the valence and structure changes in UO_2 powder samples heated in-situ in O_2 from 300 to 970 K. The peak of HERFD-XAS at 300 K had the same shape as UO_2. At 470 K, the peak became broadened, with the disappearance of the sub-peak just after the main peak. The HERFD-XAS of UO_2 at 520 K was basically the same as that at 470 K, indicating that the oxidation process could not be maintained at lower temperatures, though some authors found that UO_2 powder above 470 K was transformed to U_3O_7/U_4O_9 or similar structure [21]. At 620, 770 and 970 K, the HERFD-XAS spectra, without substantial changes, are similar to U_3O_8.

Powder diffraction patterns of the sample before and after oxidation are shown in Fig. 4. In Fig. 4a, at room temperature, the diffraction patterns are of characteristic diffraction peaks corresponding to the UO_2 structure (PDF-65-0285), while after oxidation (Fig. 3b), the diffraction patterns show the same peak positions to U_3O_8 structure (PDF-47-1493), indicating the transform from UO_2 to U_3O_8.

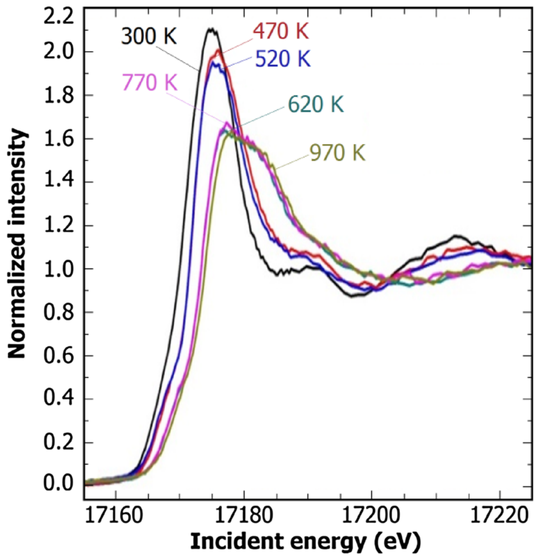

Fig. 3 HERFD-XAS of UO_2 at different temperatures

4 Conclusion

The in-situ HERFD-XAS of UO_2 oxidation is helpful in analyzing complex products in oxidation process and providing precise XAS of U L_3-edge. The in-situ high-energy-resolution X-ray absorption spectroscopy technology has been established successfully at SSRF. From the HERFD-XAS of UO_2 samples heated in-situ to 300–970 K and oxidized for 1 h, the variation of valence states can be described and the changes in crystalline structure can be

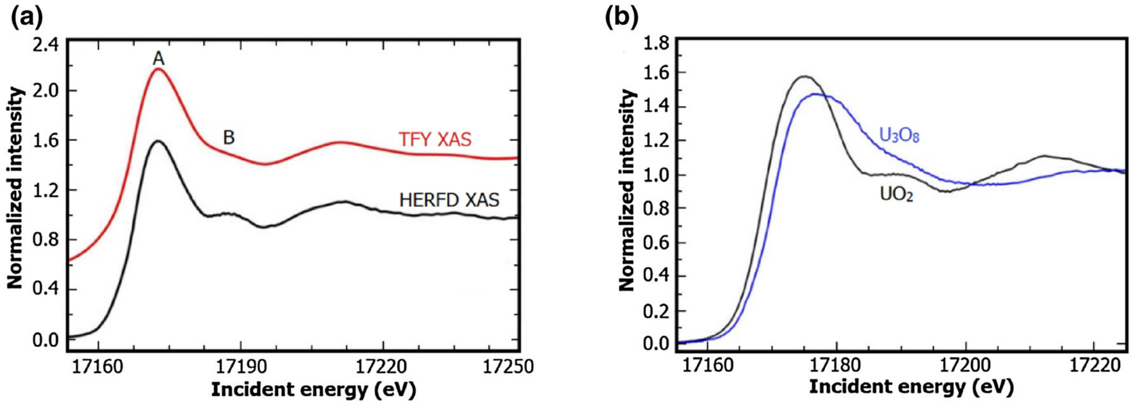

Fig. 2 U L_3-edge HERFD-XAS and TFY-XAS of UO_2 (**a**) and HERFD-XAS of UO_2 and U_3O_8 (**b**)

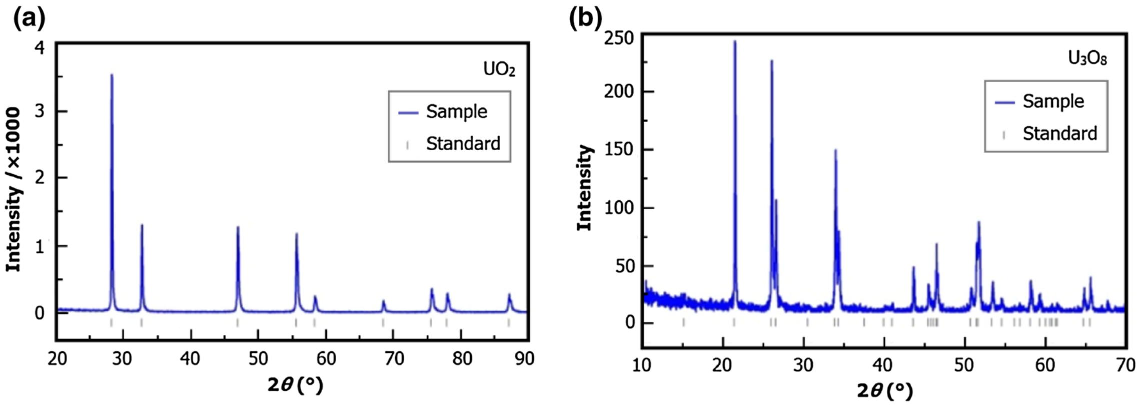

Fig. 4 Powder XRD patterns of the sample at room temperature (**a**) and after the oxidation process (**b**)

deduced. Temperature is basically the decisive factor in the oxidation process. The HERFD-XAS indicated structural changes agree with previous reports by other methods.

References

1. R.J. McEachern, P. Taylor, A review of the oxidation of uranium dioxide at temperatures below 400 °C. J Nucl Mater. **254**, 87–121 (1998). doi:10.1016/S0022-3115(97)00343-7
2. L. Desgranges, G. Baldinozzi, G. Rousseau et al., Neutron diffraction study of the in situ oxidation of UO(2). Inorg Chem. **48**, 7585–7592 (2009). doi:10.1021/ic9000889
3. W.Q. Shi, L.Y. Yuan, C.Z. Wang et al., Exploring actinide materials through synchrotron radiation techniques. Adv Mater. **26**, 7807–7848 (2014). doi:10.1002/adma.201304323
4. T. Prüßmann, M.A. Denecke, A. Geist et al., Comparative investigation of N donor ligand-lanthanide complexes from the metal and ligand point of view. J Phys Conf Ser. **430**, 012115 (2013). doi:10.1088/1742-6596/430/1/012115
5. C.H. Booth, Y. Jiang, D.L. Wang et al., Multiconfigurational nature of 5f orbitals in uranium and plutonium intermetallics. Proc Natl Acad Sci USA. **109**, 10205–10209 (2012). doi:10.1073/pnas.1200725109
6. T. Vitova, M.A. Denecke, J. Göttlicher et al., Actinide and lanthanide speciation with high-energy resolution X-ray techniques. J Phys Conf Ser. **430**, 012117 (2013). doi:10.1088/1742-6596/430/1/012117
7. K.O. Kvashnina, Y.O. Kvashnin, S.M. Butorin, Role of resonant inelastic X-ray scattering in high-resolution core-level spectroscopy of actinide materials. J Electron Spectrosc Relat Phenom. **194**, 27–36 (2014). doi:10.1016/j.elspec.2014.01.016
8. C.J. Nelin, P.S. Bagus, E.S. Ilton, Theoretical analysis of the U L3-edge NEXAFS in U oxides. RSC Adv. **4**, 7148 (2014). doi:10.1039/c3ra46738d
9. K. Kvashnina, Y. Kvashnin, J.R. Vegelius et al., Sensitivity to actinide doping of uranium compounds by resonant inelastic X-ray scattering at uranium L-3 Edge. Anal Chem. **87**, 8772–8780 (2015). doi:10.1021/acs.analchem.5b01699
10. J.G. Tobin, S.W. Yu, R. Qiao et al., Covalency in oxidized uranium. Phys Rev B. (2015). doi:10.1103/PhysRevB.92.045130
11. A. Walshe, T. Prussmann, T. Vitova et al., An EXAFS and HR-XANES study of the uranyl peroxides [UO2(eta2-O2)(H2O)2]·nH2O (n = 0, 2) and uranyl (oxy)hydroxide [(UO2)4O(OH)6]·6H2O. Dalton Trans. **43**, 4400–4407 (2014). doi:10.1039/c3dt52437j
12. T. Vitova, K.O. Kvashnina, G. Nocton et al., High energy resolution X-ray absorption spectroscopy study of uranium in varying valence states. Phys Rev B. (2010). doi:10.1103/Physrevb.82.235118
13. J.G. Tobin, S.W. Yu, C.H. Booth et al., Oxidation and crystal field effects in uranium. Phys Rev B (2015). doi:10.1103/PhysRevB.92.035111
14. X.-D. Wen, M.W. Löble, E.R. Batista et al., Electronic structure and O K-edge XAS spectroscopy of U3O8. J Electron Spectrosc Relat Phenom. **194**, 81–87 (2014). doi:10.1016/j.elspec.2014.03.005
15. X. Gao, S. Gu, Q. Gao et al., A high-resolution X-ray fluorescence spectrometer and its application at SSRF. X-Ray Spectrom. **42**, 502–507 (2013). doi:10.1002/xrs.2511
16. H.S. Yu, X.J. Wei, J. Li et al., The XAFS beamline of SSRF. Nucl Sci Tech. **26**, 050102 (2015). doi:10.13538/j.1001-8042/nst.26.050102
17. M.A. Denecke, Actinide speciation using X-ray absorption fine structure spectroscopy. Coord Chem Rev. **250**, 730–754 (2006). doi:10.1016/j.ccr.2005.09.004
18. L. Martel, J.-F. Vigier, D. Prieur et al., Structural investigation of Uranium–Neptunium mixed oxides using XRD, XANES, and 17O MAS NMR. J Phys Chem C. **118**, 27640–27647 (2014). doi:10.1021/jp507088t
19. S.D. Conradson, D. Manara, F. Wastin et al., Local structure and charge distribution in the UO2-U4O9 system. Inorg Chem. **43**, 6922–6935 (2004). doi:10.1021/ic049748z
20. K.O. Kvashnina, S.M. Butorin, P. Martin et al., Chemical state of complex uranium oxides. Phys Rev Lett. **111**, 253002 (2013). doi:10.1103/PhysRevLett.111.253002
21. P.E. Blackburn, J. Weissbart, E.A. Gulbranson, Oxidation of uranium dioxide. J Phys Chem. **62**, 902–908 (1958). doi:10.1021/j150566a002